Supporting information

Giant enhancement of luminescence down-shifting by a doubly-resonant rare-earth-doped photonic metastructure

Ngoc-Vu Hoang,[†,*] Antonio Pereira,[†,*] Hai Son Nguyen,[‡] Emmanuel Drouard,[‡] Bernard Moine,[†] Thierry Deschamps,[‡] Regis Orobtchouk,[§] Anne Pillonnet,[†] Christian Seassal[‡,*]

[†]*Univ Lyon, Université Claude Bernard Lyon 1, CNRS, Institut Lumière Matière, F-69622, Villeurbanne, France*

[‡]*Univ Lyon, Institut des Nanotechnologies de Lyon - INL, UMR CNRS 5270, CNRS, Ecole Centrale de Lyon, Ecully F-69134, France*

[§]*Univ Lyon, Institut des Nanotechnologies de Lyon - INL, UMR CNRS 5270, CNRS, INSA de Lyon, Villeurbanne F-69621, France*

1. Design of the 2D photonic crystal: figure of Merit (FOM)

The PC structure has been optimized with a view to maximize the absorption of sunlight by the active medium (through its excitation spectrum), and considering the best possible photonic structures through its ability to control. These criteria have been formalized in a figure of merit presented below. In our design, a square symmetry of air holes was chosen. The PC structural parameters, including the SiN_x thickness t, the lattice period p, and the aspect ratio D/p (D being the holes diameter), were varied

to ensure high absorption in the DSL. The thickness of the DSL was set to 100 nm, and the optical properties (n, k) of each material were derived from spectroscopy ellipsometry measurements. The influence of the PC structural parameters on the absorption of the DSL layer is summarized with the figure of merit (FOM). The FOM was calculated as follows

$$FOM = \int A(\lambda).PLE(\lambda).S(\lambda).d\lambda$$

where $A(\lambda)$ is the absorption spectrum of the device which is numerically calculated by the RCWA method (RCWA), $PLE(\lambda)$ is the experimental photoluminescence excitation spectrum of Eu^{3+} (see Figure 2a), and $S(\lambda)$ is the solar spectrum. As shown in Figure SI.1, regions characterized by a high absorption are observed for p = 247 - 252 nm and D/p = 0.64 - 0.74 (the SiN_x thickness was t = 100 nm). In that case, two resonant modes in the range 390-430 nm are generated, and a drastic enhancement of absorption in the DSL is therefore expected.

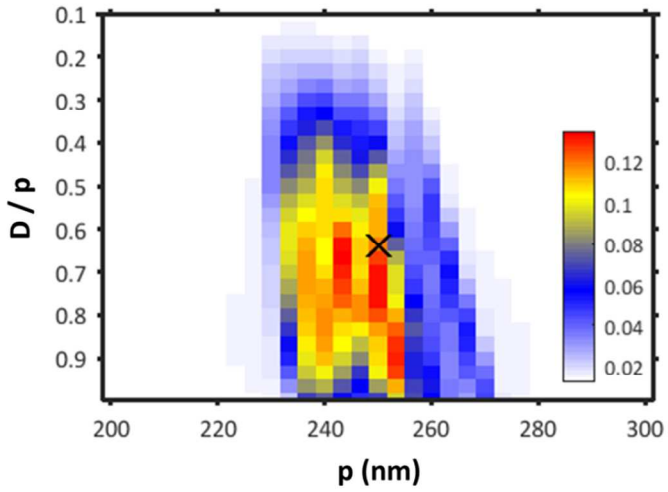

Figure SI.1 Figure of Merit for the new down-shifting structure calculated by scanning the PC geometrical parameters (t = 100 nm, p = 200 - 300 nm and D/p = 0 - 1).

2. Fabrication the new metastructure

As explained in the main text, we used different-nanofabrication steps to fabricate the new photonic metastructure. Figure SI.2 depicts the fabrication process which can be divided into two parts: the conversion layer elaboration and the photonic crystal fabrication.

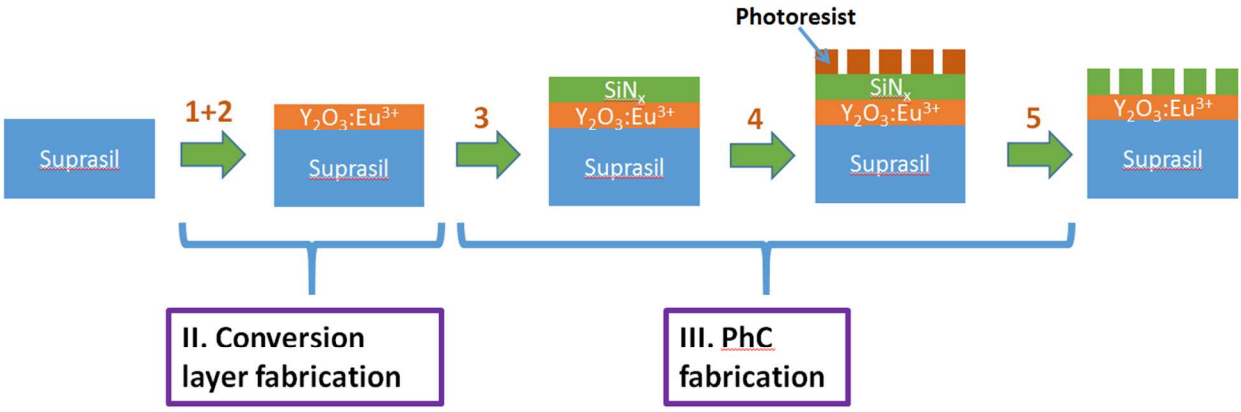

Figure SI.2 Scheme of the fabrication process that combines pulsed laser deposition for the DSL, and frequency plasma enhanced chemical vapor deposition, laser interference lithography and reactive ion etching for the PC.

3. Characterization of the conversion layer

To control the crystallization of Y_2O_3:Eu^{3+} thin films after annealing, x-ray characterization was performed using a Rigaku SmartLab diffractometer with a $CuK_{\alpha 1}$ radiation (λ = 1.5406 Å) in the θ-2θ Bragg-Brentano configuration. Diffractograms were carried out with a 0.01° step size and a scan speed of 2^{o}/min. The diffractogram depicted in Figure SI-3a shows a series of diffraction peaks located at 29.17° (222), 33.93° (400), 48.54° (440) and 57.79° (622). This agrees well with the peak position expected for Y_2O_3 (JCPDS-ICCD card no. 00-025-1200). The peak positions do not shift toward larger 2θ values by more than 0.2°, indicating that the structure of the Y_2O_3 matrix is slightly modified by the europium doping. The deduced lattice parameter a_{hkl} obtained from the main diffraction peaks is 10.583 Å, which corresponds well to the value found in the literature (JCPDS-ICCD card no. 00-025-1200). The surface morphology of the films was also investigated by atomic force microscopy (AFM, Asylum

Research) in tapping mode with a scan rate of 2 Hz. Commercial non-contact AFM probes (Tap190Al-G, Budgetsensors) were used to scan the surface. Three different areas on the sample (5 µm x 5 µm) were scanned to obtain an average value of the root mean square roughness (RMS). Typical AFM image is shown in Figure SI.3b. A continuous layer without cracks is evidenced. The average roughness is found to be ~ 0.57 nm, which is comparable to that of the substrate (RMS = 0.62 nm).

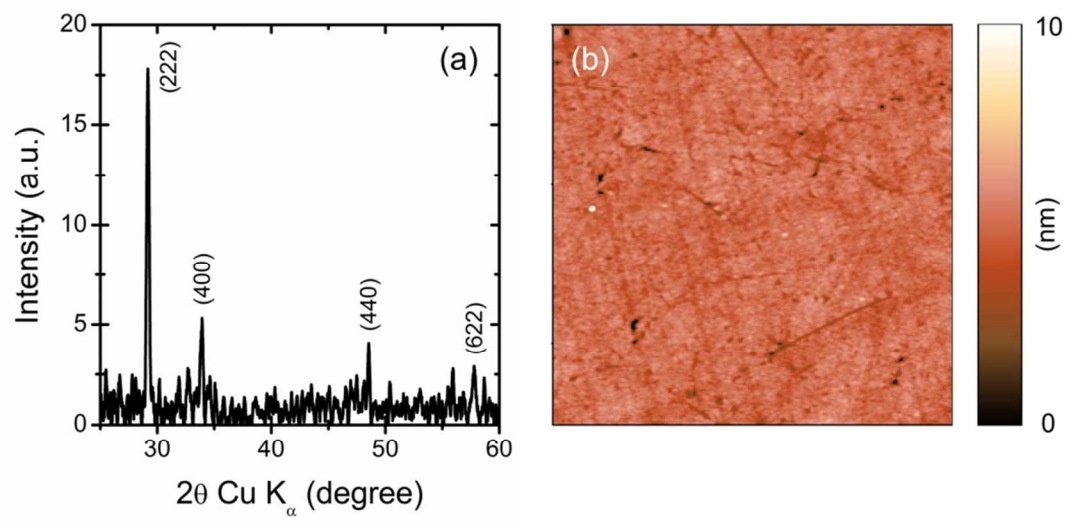

Figure SI.3 (a) X-ray diffractogram of annealed Y_2O_3:Eu^{3+} thin film, and (b) the corresponding AFM image (5 x 5 µm).

Figure SI.4a shows the transmittance spectra of the Y_2O_3: Eu^{3+} layer before and after annealing, recorded using a UV-VIS spectrophotometer (Lambda900 from Perkin-Elmer). After annealing, the average transmittance above 350 nm reaches ~ 84%, indicating a highly transparent layer. Spectroscopic ellipsometry (UVISEL from Horiba Jobin-Yvon) was used to determine the optical properties (refractive index n and the extinction coefficient k) of the annealed Y_2O_3: Eu^{3+} thin film. Optical measurements were taken between 250 and 800 nm at an incident angle of 70°. Optical properties were then derived using single Lorentz oscillator model to fit the measured ellipsometric data. Figure SI.4b shows the dependence of n and k as a function of the wavelength. The calculated refractive index and extinction coefficient vary from 2.05 to 1.84 and from 10.61 x 10^{-3} to 1.38 x 10^{-3}

over the 250 - 800 nm spectral range, respectively. These values are in agreement with the literature.[1-3] The slight discrepancies are related to the doping concentration and to the method of fabrication.

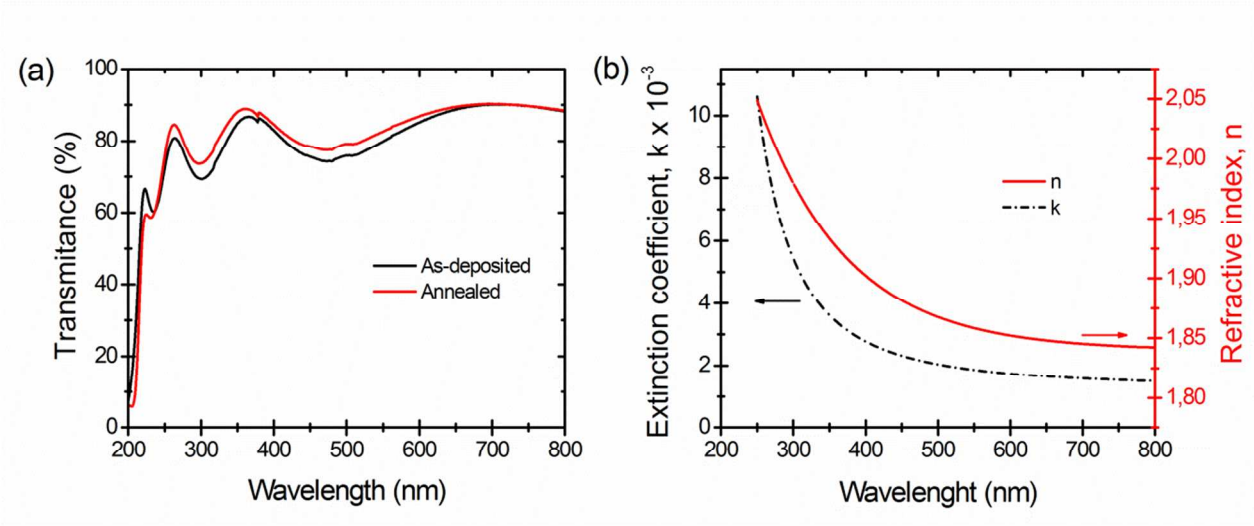

Figure SI.4 Optical properties of the Y_2O_3:Eu^{3+} thin film: (a) transmittance before and after annealing, (b) optical constants (n and k) for the annealed film.

4. Optical properties of the SiN_x layer

A 100-nm thick SiN_x layer was deposited on the top of Y_2O_3: Eu^{3+} by low-frequency plasma-enhanced chemical vapor deposition. The SiN_x stoichiometry was controlled by adjusting the SiH_4/NH_3 gas ratio. The optical properties of SiN_x were determined by ellipsometric measurements to ensure the low extinction coefficient k ($< 10^{-6}$ for $\lambda \geq 350$ nm) and the proper refractive index n in the working spectrum (Figure SI.5).

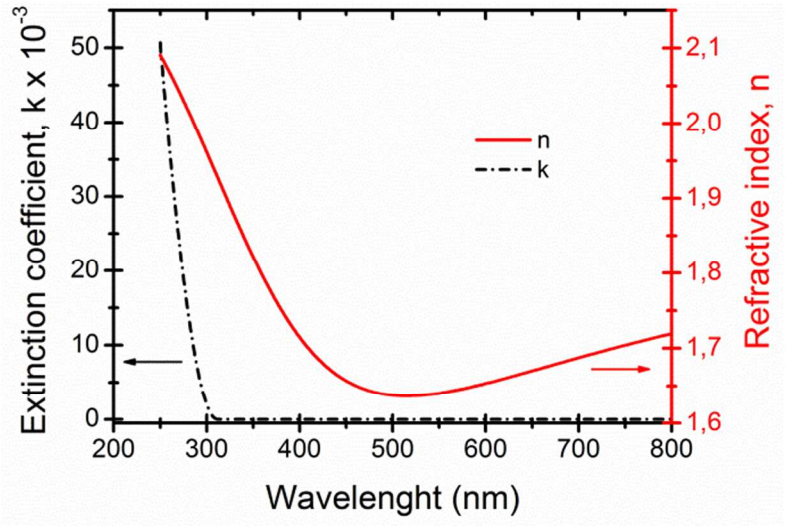

Figure SI.5 Optical constants (n and k) for the SiN_x thin film.

5. SEM image of the fabricated PC structure and calculation of the diameter distribution of the holes

The homogeneity of new meta-structure is examined by scanning electronic microscopy (SEM). 25 images with a resolution of 5 µm x 5 µm were captured within 1 mm x 1 mm area and the distance between 2 images was 0.25 mm (Figure SI.6a). Diameter distribution of each image is then determined by ImageJ program and integrated into diameter histogram in the area 1 mm x 1 mm (Figure SI.6b).

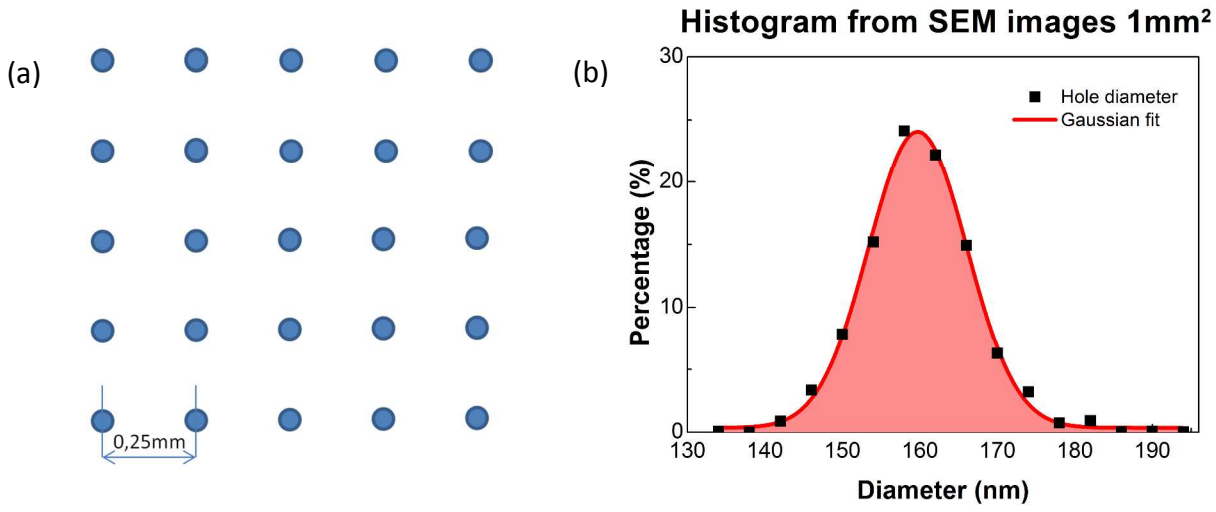

Figure SI.6 (a) SEM mapping on 1 mm x 1 mm, and (b) histogram of radius distribution.

6. Bloch modes of the photonic structure at 400 nm and 611 nm

The dispersion diagram of Bloch modes of the metastructure is theoretically calculated with the use of the commercial software RSOFT (Figure SI.7). We distinguish clearly slow modes at 400 nm at the Γ point, and fast modes above the light line at 611 nm along Γ–X direction (i.e. ϕ =0). These are the photonic modes responsible respectively to the absorption enhancement at 400 nm and extraction enhancement at 611 nm as discussed in the main text. Note that Bloch modes at 611 along Γ–M direction (i.e. ϕ =0) is below the light line and do not participate to the extraction enhancement. The extraction enhancement for different angle ϕ is discussed in detail in the section 7.

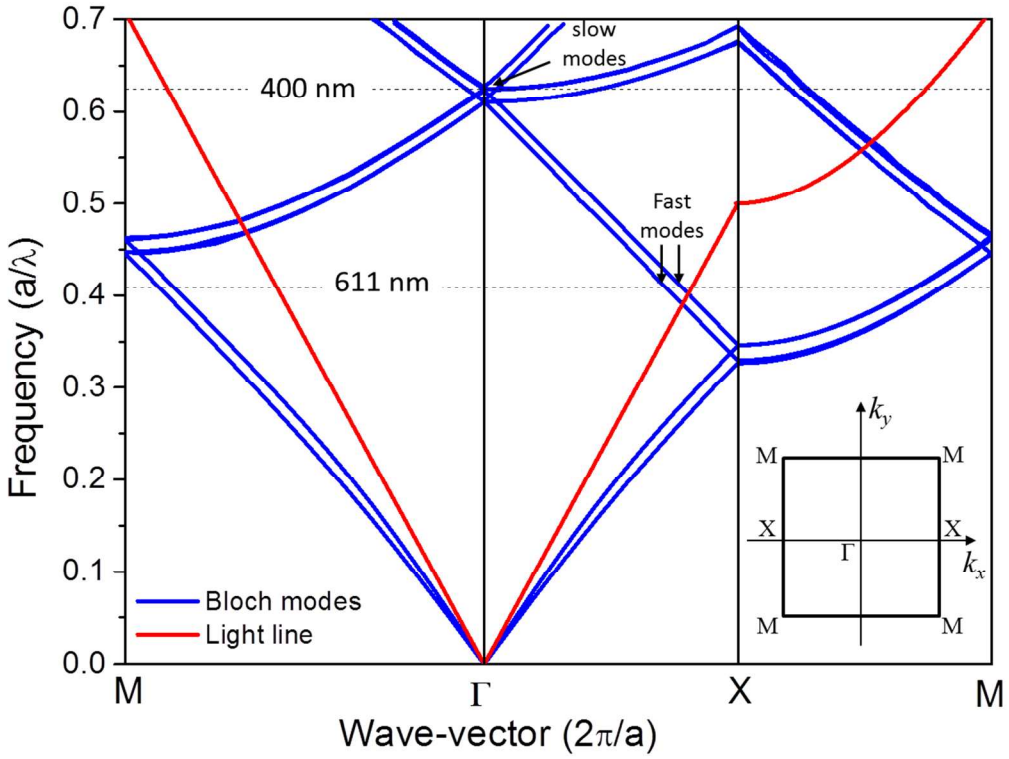

Figure SI.7 Theoretical calculation of the dispersion diagram of Bloch modes of the metastructure.

7. Extraction enhancement for different in-plane directions

The photoluminescence image in the Fourier space is captured onto the sensor of a CCD camera (Syncerity, Horiba) which is coupled to a spectrometer (microHR, Horiba) (Figure SI.8). The

horizontal coordinate of each pixel corresponds to an emission wavelength and the vertical one corresponds to an emission angle θ. This setup is in reflection geometry and only allows analyzing the front emission. Compared to the angular resolved experiment presented in the main text, this experiment measures in one shot (few seconds of integration time) the front emission pattern within the numerical aperture of the microscope objective (NA = 0.42) for a given angle ϕ. Since the emission pattern is in oblique angles, an offset by inclining the sample 65° is introduced.

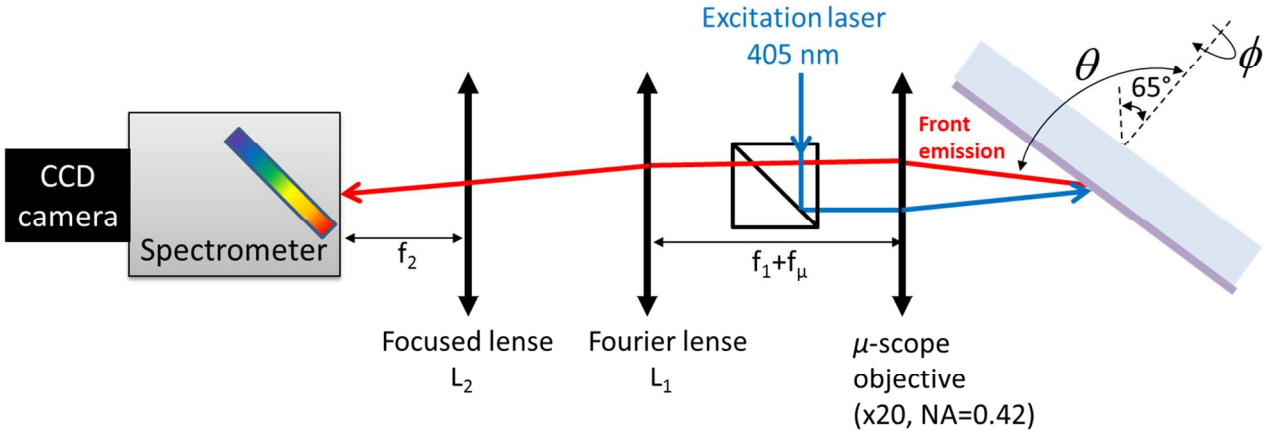

Figure SI.8 Experimental setup for imaging the front emission pattern on to a CCD sensor.

The front emission pattern is measured with ϕ varying from 0 to 45 degrees with step of 3 degrees. Several representative results are presented in Figures SI.9a-e. From these measurements, the photoluminescence intensity at 611 nm as a function of θ and ϕ is extracted (Figure SI.9f). We observe experimentally that:

- for $\phi < 15°$, both of two fast modes at 611 nm are above the light line and enhance the emission extraction;
- for $15° < \phi < 24°$, only one of the two fast modes at 611 nm is above the light line and enhances the emission extraction;

- for $\phi > 24°$, both of two fast modes at 611 nm are below the light line and there is no enhancement of the emission extraction.

Figure SI.9g depicts the simulation results obtained by RCWA. The simulation reproduces qualitatively well the experimental features. The different of values of ϕ and θ of Bloch modes at 611 nm is due to the measurements and it is attributed to the imperfect shape of the PC holes as mentioned in the main text.

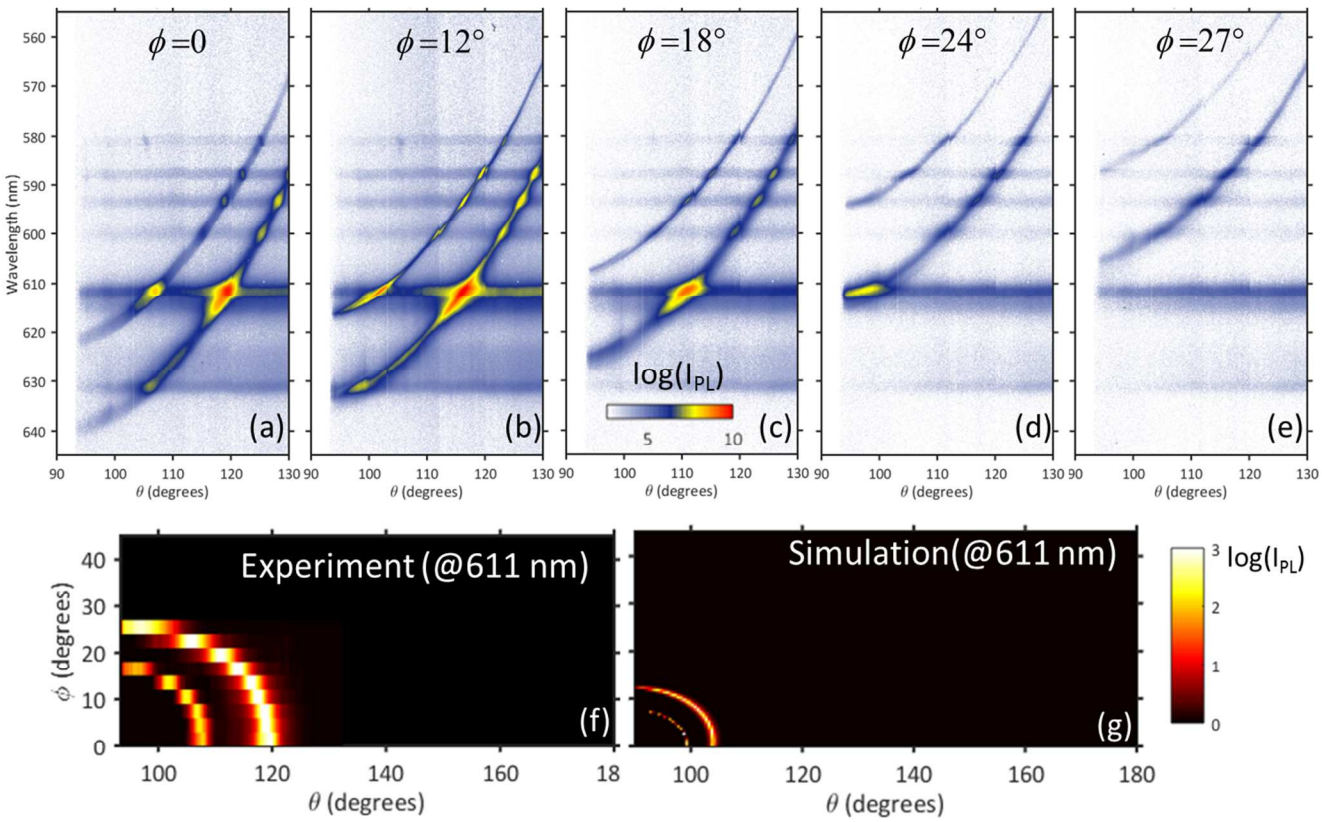

Figure SI.9 (a)-(e). Spectral and angular resolved emission pattern of the metastructure with ϕ = 0°, 12°, 18°, 24° and 27°. (f) Photoluminescence intensity of the metastructure at 611 nm as a function of ϕ and θ. (g) Simulation result of f).

8. Lifetime measurements

Luminescence decay time is also measured inside the integrating sphere under normal incident laser excitation and using the same experimental setup described in section 6. We observed that the lifetime of metastructure sample is nearly unchanged compared to reference sample (Figure SI.10). The difference observed (~ 4%) is within the experimental error.

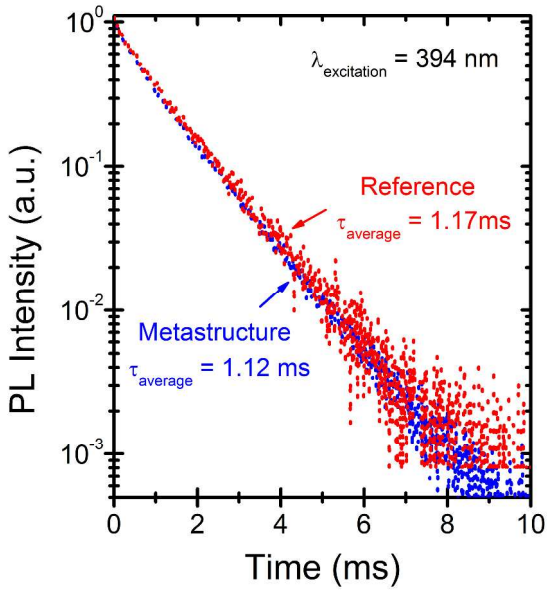

Figure SI.10 Luminescence decay time of the metastructure and reference samples.

REFERENCES

1. Nigara, Y. Measurement of the Optical Constants of Yttrium Oxide. *Jpn. J. Appl. Phys.* **1968**, *7*, 404-408.
2. Palik, E. D. *Handbook of Optical Constant of Solid II*, Academic Press: Orlando, 1998; pp. 1079.
3. Wang, X. J.; Zhang, L. D.; Zhang, J. P.; He, G.; Liu, M.; Zhu, L. Q. Effects of Post-Deposition Annealing on the Structure and Optical Properties of Y_2O_3 Thin Films. *Mater. Letters* **2008**, *62*, 4235-4237.